Polymer Chemistry

ROYAL SOCIETY OF CHEMISTRY

PAPER

View Article Online
View Journal | View Issue

Cite this: *Polym. Chem.*, 2022, **13**, 3631

Exploiting the reversible covalent bonding of boronic acids for self-healing/recycling of main-chain polybenzoxazines†

Sevinc Gulyuz, Yusuf Yagci and Baris Kiskan *

In this work, a new strategy for the synthesis of self-healable/recyclable polybenzoxazine networks under mild conditions by exploiting dynamic B–O bond exchanges is presented. The process is based on mixing main chain polybenzoxazine precursors with phenyl boronic acid and heating up to 180 °C. The obtained polybenzoxazine films displayed good self-healing properties at low temperatures and very mild pressures in the absence of additives to promote the healing process. The recovery extent of the films was quantified by tensile tests. The stress relaxation and sweep frequency behaviour of the films were analyzed by rheological measurements. The spectral and thermal behaviors of the films were also investigated. Moreover, the networks showed higher hydrolysis stability than those of conventional boronic esters because of the intramolecular coordination of B–N in the linkages.

Received 17th January 2022,
Accepted 19th May 2022

DOI: 10.1039/d2py00068g

rsc.li/polymers

Introduction

Polybenzoxazines (PBzs) have emerged as contender thermosets to classical phenol-formaldehyde (PF) resins in the last two decades. PBzs exhibit unusual properties unlike PF resins such as low water adsorption, limited cure shrinkage, low by-product formation during curing, non-catalytic polymerization and less brittleness depending on the functionalities present on PBzs.[1] In addition to these unique characteristics, they produce char with high yields and have high glass transition temperatures (T_g) and for some PBzs, T_g can even be higher than their curing temperatures.[2] Therefore, research interest in PBzs and related materials is apparently increasing in polymer and materials science as reflected by the number of scientific publications and patents.[3] Many of the above-stated properties are due to the chain conformations arising from Mannich base bridges (–CH_2–N(R)–CH_2–), and the intra- and intermolecular hydrogen bonds between amine and phenolic –OH groups.[4]

PBzs are obtained from their corresponding 1,3-benzoxazine (Bz) monomers and the polymerization proceeds by a thermally driven cationic ring opening process (ROP) under either catalytic or non-catalytic conditions. Typically, the ROP temperatures of Bz monomers lie between 180 to 250 °C depending on the substituents on Bz and the purity of the monomer[5] used if the process is non-catalytic.[6–11] Another important advantage of PBzs over many other resins is the rapidly expanding monomer library.[12–16] A typical Bz monomer synthesis involves the use of a suitable primary amine, a phenolic compound and formaldehyde.[17–20] These components can be modified to obtain designed Bzs to regulate the final physical and chemical properties of the PBz therefrom. Hence, benzoxazine chemistry offers a large number of monomer options matching with the application purposes. Particularly, smart materials can be designed using carefully selected benzoxazines, which bear specific functionalities.[21] It is also possible to impart dynamic covalent bonding sites on PBzs or supramolecular interactions to produce self-healable materials.[22–24] For example, self-healing by light triggered [2 + 2] cycloaddition was accomplished using coumarin functional benzoxazines.[25] Although deep light penetration into such materials is limited, these systems were shown to be capable of initiating the healing process on demand. In contrast to systems dependent on external stimulation, autonomic self-healable PBzs were reported. Self-healing based on supramolecular interactions was shown by using –COOH functional benzoxazines through increased H bonding in the PBz network.[26] In another example, a main-chain polybenzoxazine precursor was used as the healing agent for polysulfones.[27] Alternatively, a thermally triggered S–S bonding/de-bonding approach was also applied to design recyclable polybenzoxazines. With this approach, poly(benzoxazine-*co*-sulfides) were synthesized with high sulfur contents by the inverse vulcanization process.[28] Here, it should be noted that benzoxazines are known as the sole monomer type that could undergo inverse

Istanbul Technical University, Department of Chemistry, 34469, Maslak, Istanbul, Turkey. E-mail: kiskanb@itu.edu.tr

† Electronic supplementary information (ESI) available. See DOI: https://doi.org/10.1039/d2py00068g

vulcanization[29–31] apart from vinylics and other resembling monomers.[32,33] Similar sulfur chemistry was used to produce cardanol-based polybenzoxazine vitrimers.[34] Moreover, a transesterification reaction was successfully employed to create catalyst-free polybenzoxazine vitrimers.[35] A $Zn(OAc)_2$ catalyzed transesterification approach was also reported and thermally assisted self-healing on the surface of polybenzoxazines was successfully achieved.[36] In a different study, PBzs from *ortho*-blocked bifunctional benzoxazines exhibited vitrimer properties and the networks could be remolded from crushed pieces or healed from mechanical damage.[37] Recently, the dynamism of Si–O–Ph linkages was used to produce reprocessable and degradable PBz thermosets. For this purpose, a siloxane containing monofunctional benzoxazine was synthesized and then oligomers were obtained therefrom. The oligomers were hot pressed for crosslinking by a $Si–OCH_3$/Si–OPh exchange reaction. The final product could be reprocessed at 250 °C and under 10 MPa pressure.[38] Apparently, the unique hydrogen bonding of PBzs also contributed to self-healing processes besides dynamic covalent bonding in all the reports stated above.[4] In brief, a PBz system can be considered as an inherently supramolecular material having the potential to fabricate self-healable materials by a specific design. Accordingly, organoboron-bearing PBzs can be produced for self-healing, recycling, and reprocessing purposes since organoboron containing polymers manifest a number of interesting properties including B–O bond reversibility.[39,40] Selected organoboron species make them highly useful in reversible crosslinks for the design of healable/reprocessable bulk polymers. Symmetric vitrimers based on dioxaborolane metathesis,[41] 3D-printed dynamic covalent networks based on boronate esters,[42] strong, highly malleable, and recyclable thermosetting materials based on boroxines,[43] room-temperature healing based on boronic ester network materials obtained by photoinitiated thiol–ene curing,[44] and self-healing polymers obtained by bond exchange in boronic esters with neighboring hydroxyls[45] can be given as typical examples. Other remarkable smart materials related to boroxines are solution-processable and thermostable poly(aryl ether ketone) thermosets.[46] These thermosets exhibited a tensile strength between 60 and 98 MPa with a Young's modulus from ≈4 to ≈6 GPa.

Apart from designing self-healable/reprocessable materials, B–O bonds have other benefits such as improving the thermal stability of the polymers. For example, boron modified phenolic resins and PBzs have been used in many practical applications due to their excellent oxidation resistance, high temperature stability, high char yields and improved mechanical properties related to B–O bonds.[47–52] Evidently, the phenolic –OH functionality of PBzs could easily react with boronic acids/esters and B–O bond linkages occur in the network structure. Thus, it is possible to exploit the dynamic behavior of these B–O bonds to create self-healable/reprocessable PBz materials. In this study, this possibility is investigated and the results clearly disclose that curing main-chain polybenzoxazines with phenyl boronic acid ($PhB(OH)_2$) could form elastic and self-healable PBz films. These films could be recycled several times at relatively low temperatures and pressures such as 110 °C and much less than one MPa, which could be considered as a significant advancement compared to similar boronic ester vitrimers.

Experimental

Materials

4,4′-Isopropylidenediphenol (bisphenol A) (Aldrich, 97%), paraformaldehyde (Sigma-Aldrich, powder, 95%), *O*,*O*′-bis(2-aminopropyl) polypropylene glycol-*block*-polyethylene glycol-*block*-poliproylene glycol (Jeffamine ED-900 or PPO_{900}, Aldrich), *O*,*O*′-bis(2-aminopropyl) polypropylene glycol-*block*-polyethylene glycol-*block*-polypropylene glycol (Jeffamine ED-600 or PPO_{600}, Aldrich), phenylboronic acid (Aldrich, 95%), *para*-cresol (Sigma-Aldrich, 99%), benzylamine (Thermo Scientific, 99.5+%), ethanol (Honeywell, ≥99.8%), toluene (Merck), *N*,*N*-dimethylformamide (DMF, Sigma-Aldrich, ≥99.8%), dimethyl sulfoxide (DMSO, Sigma-Aldrich, ≥99.9%), 1,4-dioxane (Sigma-Aldrich, ≥99.0%), acetone, ethyl acetate, tetrahydrofuran (THF, Supelco, ≥99.5%), chloroform (Honeywell, 99.0–99.4%), and *n*-hexane (Aldrich, 95%) were used as received.

Measurements

^1H NMR spectra were recorded on an Agilent NMR System VNMRS 500 spectrometer at room temperature in $CDCl_3$ or DMSO-d_6 with $Si(CH_3)_4$ as an internal standard. Fourier-transform infrared (FT-IR) spectra were recorded on a PerkinElmer FTIR spectrum one spectrometer. Gel permeation chromatography (GPC) analyses were performed using a TOSOH EcoSEC GPC system including an autosampler system, a column oven, a temperature-controlled pump, a degasser unit, a TSKgel superhZ2000 4.6 mm ID × 15 cm × 2 cm column and a refractive index detector. As an eluent, tetrahydrofuran (THF) was used with a flow rate of 1.0 mL min^{-1} at 40 °C. A refractive index detector was calibrated with polystyrene standards, which have a narrow molecular-weight distribution. Eco-SEC analysis software was used to analyze the data obtained from SEC (size-exclusion chromatography). Differential scanning calorimetry (DSC) was performed on a PerkinElmer Diamond DSC from 30 °C to 320 °C with a heating rate of 10 °C min^{-1} under a nitrogen flow. A typical DSC sample was 2–5 mg in a 30 μL aluminum pan. Thermogravimetric analysis (TGA) was performed on a PerkinElmer Diamond TA/TGA with a heating rate of 10 °C min under a nitrogen flow. Uniaxial elongation measurements were performed at 23 ± 2 °C on the samples using a Zwick Roell test machine with a 500 N load cell. Rheology experiments were performed on an Anton Paar MCR 302 using the disk type specimen with a size of about 15 ± 1 mm in diameter and 1 ± 0.11 mm in thickness. The relaxation modulus (G) was monitored over time. The sample was equilibrated at the setting temperature for 15 min, and 1% strain was applied. Normalization of the data (G/G_0) was performed to obtain stress relaxation curves. Frequency sweep experiments were performed in the frequency range of

0.01–100 rad s^{-1} with a strain of 0.2%. The storage (G') and loss (G'') moduli were consequently plotted as a function of frequency.

Synthesis of poly(propylene oxide)benzoxazines (PPO_{600}-Bz and PPO_{900}-Bz)

In a 250 mL round bottomed flask, paraformaldehyde (32.0 mmol, 0.96 g), bisphenol A (8.32 mmol, 1.90 g), and poly (propylene/ethylene oxide) bisamine (PPO_{600} or PPO_{900}) (8.0 mmol) were dissolved in a 50 mL toluene and 25 mL ethanol mixture. The reaction mixture was refluxed for 24 h. The solvent was evaporated under vacuum, and a blondish oily product was precipitated in cold *n*-hexane. The reprecipitation process was performed three times. The final product was dried at room temperature in a vacuum for 3 days.

Film preparation

PPO-Bz-Bor films with 10% wt phenyl boronic acid ($PhB(OH)_2$) content were prepared. $PhB(OH)_2$ and PPO-Bz-Bor were mixed with 10 mL of chloroform in a 20 mL beaker and charged into a Teflon mold. The solvent was evaporated at room temperature for 3 days and then solvent residues were removed by keeping the molds under vacuum for 1 day. Then, the film mixture was exposed to thermal curing starting from 110 °C to 180 °C for 2 h in an oven (with a heating ramp of *ca.* 5–6 °C per 10 min). Finally, brownish and transparent polybenzoxazine cross-linked films were obtained.

Results and discussion

It is well known that the B–O bonds in boronic esters exhibit bond exchange dynamism through both dissociative and associative pathways. Boronic esters first hydrolyze to diols and boronic acids and then undergo re-esterification with complementary reaction partners to reform new B–O linkages in the dissociative mechanism. In contrast, in the associative pathway, instead of complete hydrolysis, the average number of B–O bonds is sustained by transesterification with another free hydroxyl, which should be excess in the designed material.[44,53,54] In both pathways, the boronic ester exchange can be tuned by neighboring groups and self-healing efficiencies could be improved *via* rapid exchange reactions. For example, a basic nitrogen atom located at a favorable distance from the boronic ester can cause an acceleration of bond exchange as compared to that of the non-substituted one.[55] A series of reports have been published related to tuning the dynamic exchange of boronic esters or boroxines by introducing amines as neighboring groups.[56–59] The PBz structure contains both phenolic hydroxyl, for boronic ester formation, and a basic nitrogen atom in Mannich bridges suitable for accelerating the bond exchange. Hence, the inherent structure of PBz is quite convenient to design self-healable/recyclable networks based on boronic ester exchange reactions.

Accordingly, main chain polybenzoxazines were synthesized using bisphenol A, jeff amines and paraformaldehyde for the stated purpose (Scheme 1). Two different amino end functional poly(oxy ethylene/propylene)s were selected as jeffamine 900 ($M_n \approx 900$ Da) and jeffamine 600 ($M_n \approx 600$ Da) to impart flexible units since efficient chain entanglement is crucial in a self-healable material. The obtained polymers were abbreviated as PPO_{900}-Bz and PPO_{600}-Bz according to the used jeffamine. The molecular structures of PPO_{900}-Bz and PPO_{600}-Bz were confirmed by ^{1}H NMR and FTIR spectroscopy (Fig. S1–S4†). In brief, the characteristic proton signals of N–CH_2–O and N–CH_2–Ar bridges of the oxazine ring are detected at *ca.* 4.83 ppm and 3.93 ppm for both polymers. Moreover, the fundamental IR band related to the oxazine ring mode at *ca.* 927 cm^{-1}, trisubstituted benzene C=C vibration at 1498 cm^{-1} and the C–O stretching vibration band at *ca.* 1096 cm^{-1} corresponding to the polyether moiety confirm the structures of PPO-Bz polymers. In addition to spectral analysis, the number average molecular weights of the polymers were determined by gel permeation chromatography (GPC) (Fig. S5†). M_n is *ca.* 10 720 Da for PPO_{900}-Bz and 7035 Da for PPO_{600}-Bz. The actual molecular weights are probably much higher as the measurements were conducted according to PSt standards.

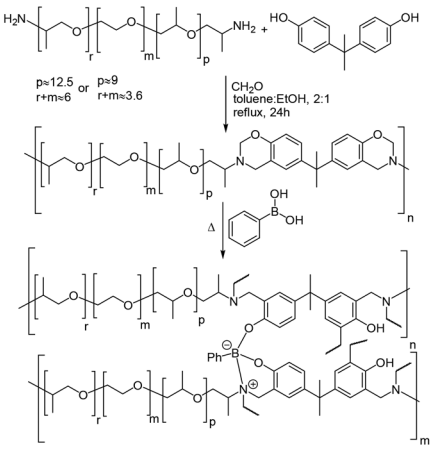

Scheme 1 Synthesis of PPO_{900}-Bz and PPO_{600}-Bz and their simultaneous curing and reactions with $PhB(OH)_2$.

As stated previously, B–O bonds are effective for constructing self-healing polymers and the unique structure of PBz is a suitable platform for designing such boronic ester based smart materials. For the ultimate goal, the chloroform solutions of PPO_{900}-Bz and PPO_{600}-Bz were simply mixed with phenyl boronic acid ($PhB(OH)_2$) (10% wt) and the solvent mixtures were cast in Teflon molds. After removal of the solvent at ambient temperature under vacuum, the films were gradually cured in an open-air oven in molds to fabricate cross-linked films (Fig. S6†). It is anticipated that $PhB(OH)_2$ reacts with the phenolic –OH groups during curing to form boronic esters and binds the PBz chains in addition to Mannich bridged linkages. Moreover, B–N interactions could also exist in the network giving a relatively weak B–N bond in this system, which could allow fast exchange reactions by slightly lengthening the B–O bonds (Scheme 1).[60,61]

The structure of the cured films was investigated by FTIR analysis. In Fig. S7,† the band at 705 cm^{-1} is attributed to the B–C bond and the band at 1560 cm^{-1} is attributed to the B–N interaction. Besides the specific bands for the boronic group, the C–O–C oxazine band located at 927 cm^{-1} in the IR spectrum (Fig. S2 and S4†) vanished, evidencing the complete curing of the PPO-Bz polymers under the stated conditions. Moreover, the broad O–H band is detectable at 3465 cm^{-1} indicating some of the –OH groups either as phenolic –OH and/or as B–OH coexisting in the network after curing. Thus, the possible B–O ester exchange between free –OH functionalities could also play a crucial role in the healing mechanism through associative pathway addition to the dissociative route. Here it should be noted that the hydroxyl band is also visible for the uncured PPO_{600}-Bz sample (Fig. S4†), indicating some ring opened structures remaining after synthesis. Actually, 100% ring closure during oxazine formation is not expected in the main-chain PBz synthesis and ring opened residual structures between 5 and 10% are common.[62–65] Besides unreacted phenolic hydroxyl groups, the poly(oxy ethylene/propylene) repeat unit has a high tendency to absorb humidity. Hence, the contribution of water in boronic ester hydrolysis and the self-healing mechanism could not be disregarded. Therefore, it could be assumed that jeffamine moieties play two distinct roles in self-healing by absorbing humidity and exhibiting essential chain mobility.

In addition to spectral analyses for the cured polymers, to provide further support related to B–N and B–O binding in a PBz, studies were carried out with a model benzoxazine monomer (C-Bn) prepared from *p*-cresol and benzylamine (Fig. S8† for the ^{1}H NMR spectrum). The C-Bn monomer produced soluble oligobenzoxazines (Oligo C-Bn) due to the blocked *para* position of the phenol. Oligo-C-Bn was reacted with $PhB(OH)_2$ under the same conditions used for the cured films (Scheme S1 and the ESI† for procedures). The obtained boron modified soluble oligomer was analyzed by ^{1}H NMR spectroscopy (Fig. S9†) and a similar spectrum was obtained as reported in a previous study related to the B–N interaction and B–O bonding in polybenzoxazines.[61] Besides spectral analyses, solubility tests were performed for the cured PPO_{900}-Bz-Bor to prove crosslinking, quantify the gel content, and determine swelling in solvents. Accordingly, pieces of the film sample were immersed in solvents for up to 7 days to observe soluble fractions and swelling. The films were practically insoluble in non-polar solvents. On the other hand, some of the polar solvents degraded the film slightly due to the water content (Fig. S10 and Table S1†). Moreover, an apparent swelling was only observed for acetone and water. The swelling ratios (J) reached their maximum values after 30 h and then a plateau is observed in the J *versus* time graph (Fig. S11†).

Regarding the stated background, the feasibility of the proposed system was tested by self-healing experiments. The cured films were cut into pieces, remolded between glass slides, tightened with metal clamps to apply mild pressure (Fig. S12†), and heated to certain temperatures in an open-air oven. In particular, while the healing experiments for PPO_{600}-Bz-Bor at 110 °C were unsuccessful, healing to some extent was observed at 140 °C. However, the mechanical strength of the healed films was deficient and the films could be detached easily by hand. The mildest conditions for effective recovery were determined as 110 °C, 5 h for PPO_{900}-Bz-Bor (Fig. 1) and as 160 °C, 5 h for PPO_{600}-Bz-Bor (Fig. S13†).

Apparently, PPO_{900}-Bz-Bor can be healed efficiently at much lower temperatures compared to PPO_{600}-Bz-Bor. The major difference between PPO_{600}-Bz-Bor and PPO_{900}-Bz-Bor is the chain length of the poly(oxy ethylene/propylene) unit and the required flexibility for effective chain entanglement at low temperatures for PPO_{600}-Bz-Bor obviously is insufficient. Accordingly, the glass temperature of the cured PPO_{900}-Bz-Bor was found to be −1.5 °C by DSC analysis (Fig. S14†). The healing efficiency of PPO_{600}-Bz-Bor, even healed at 160 °C, followed a drastic reduction trend after each cycle (Fig. S15A and S15A′). The calculated recovery efficiencies[66] are 76% for the 1st, 62% for the 3rd and 48% for the 5th healing cycle. In contrast, the recovery efficiencies for PPO_{900}-Bz-Bor increase after each cycle and start from 22% for the 1st and reach 64% for the 5th cycle (Fig. 2A and A′). Interestingly, the tensile strength of the films reduced from *ca.* 575 kPa to *ca.* 216 kPa after the 1st healing cycle and then both elongation and stress values continuously increased for each cycle. On the other hand, PPO_{600}-Bz-Bor exhibited a more usual behavior and the stress value of the films increased and the elongation decreased after each cycle, indicating a substantial increase in the rigidity of the film, possibly due to the irreversible crosslinking and side reactions at the applied temperature (160 °C). Here it could be concluded that the main structure of PPO_{900}-Bz-Bor was preserved from degradation and irreversible crosslinking reactions at low temperatures; thus a more efficient boronic ester formation took place after each cycle. It is well known that during the curing of benzoxazines, especially at low temperatures and under acidic conditions, phenoxymethyl type bridges occur, which cleave and rearrange (bind to aromatics) at high temperatures and create less flexible bonds (Scheme S2†). Accordingly, low temperature processing of PPO_{900}-Bz-Bor reduced the cleavage of phenoxymethyl type bridges[37] in the material and eliminated unwanted irreversible crosslinking. In addition, the B–N interactions seem to be pro-

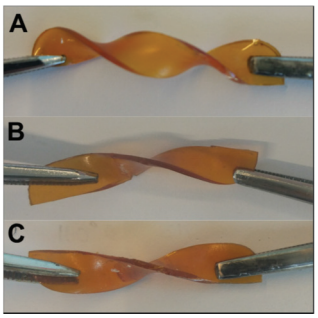

Fig. 1 Images of the cured PPO_{900}-Bz-Bor film before healing (a), after the 3rd healing cycle (b) and the 5th cycle (c).

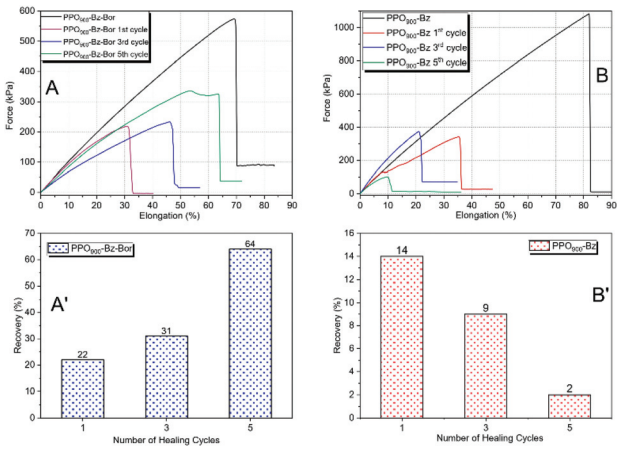

Fig. 2 Stress–strain analysis of PPO_{900}-Bz-Bor (A) and PPO_{900}-Bz (B) and the healing efficiencies of PPO_{900}-Bz-Bor (A′) and PPO_{900}-Bz (B′).

tected at low temperatures and de-polymerization over Mannich bridge cleavage subsides. In this way, the formation of cationic aminomethyl or benzylic species and additional Friedel–Crafts reactions between chains were inhibited and the rigidity of the films was not altered drastically after each healing cycle. The preservation of B–N bonds also supports the fast boronic ester exchange reactions that eventually influence the recovery ratio of the material. The structure of the PPO_{900}-Bz-Bor films after each healing cycle was analyzed by FTIR spectroscopy to reveal any significant change occurring under the used recycling conditions. The overlaid FTIR spectra (Fig. 3) of the cured PPO_{900}-Bz-Bor after the 1st, 3rd and 5th cycle did not display any observable change. Particularly, the weakest interaction in the structure was traced and the peak related to the B–N interaction at 1560 cm^{-1} remained unchanged, thus evidencing the validity of the proposed reasons for healing efficiency.

Besides, the cured PPO-Bz films were prepared under the same conditions used for PPO-Bz-Bor to show the effect of boronic esters on the healing performance. Thus, the PPO-Bz films were subjected to healing experiments under the identical conditions used for the boronic ester counterparts. Accordingly, healing was observed for both PPO_{600}-Bz and PPO_{900}-Bz to a certain extent. However, the healing efficiencies were much less than those of boronic ester samples and practically the healing after the 5th cycle halted (Fig. 2B, B′ and Fig. S15B, 15B′†). Although self-healing is limited for PPO_{600}-Bz and PPO_{900}-Bz, the observed capacity could be related to the hydrogen bonding interactions and unreacted oxazines that ring-open during healing cycles and therefore behave as an inner healing agent. Apparently, the conditions used for curing are insufficient to consume all the oxazine repeat units for PPO_{600}-Bz and PPO_{900}-Bz as determined by DSC analysis. In Fig. 4, the ring-opening exotherms of benzoxazines in the main chain are visible with a declining trend after each healing cycle, evidencing the stated reason for the observed slight healing performance of the PPO-Bz films. After each cycle, the crosslinking density increases and more phenolics are generated enhancing the brittleness and the rigidity of the films as monitored by stress–strain analysis (Fig. 2 and S14†).

In contrast, a similar curing exotherm of benzoxazines is not visible for the cured $PPO_{900\ or\ 600}$-Bz-Bor samples, indicating a complete curing process due to the catalytic effect of PhB$(OH)_2$ and excluding the contribution of the uncured oxazines for the healing mechanism (Fig. 5).

The catalytic effect of PhB$(OH)_2$ was analyzed in detail to have better insights into the curing of the PPO-Bz polymers. It is well known that acids could catalyze the ring opening of benzoxazines at low temperatures and the curing of benzoxa-

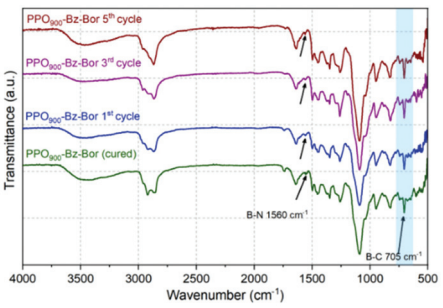

Fig. 3 FTIR spectra of the cured and recycled PPO-Bz-Bor.

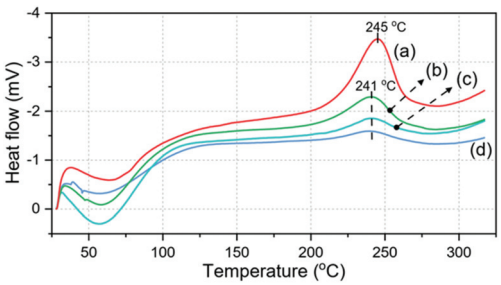

Fig. 4 DSC thermograms (endotherm down) of PPO_{900}-Bz (a), the cured PPO_{900}-Bz (b), the cured PPO_{900}-Bz after the 1st (c) and 5th (d) healings.

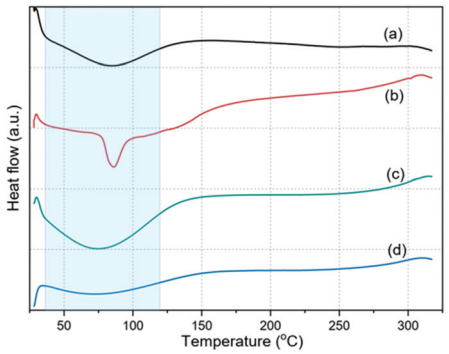

Fig. 5 DSC thermograms (endotherm down) of the cured PPO_{900}-Bz-Bor (a), and the 1st (b), 3rd (c) and 5th (d) cycles of the cured PPO_{900}-Bz-Bor.

zines can be much lower than un-catalyzed polymerization. Evidently, the catalytic effect of added $PhB(OH)_2$ is observed where the DSC thermograms of PPO_{900}-Bz and PPO_{900}-Bz/$PhB(OH)_2$ (10% wt) are sketched for comparison (Fig. S16†). The onset and the maximum curing temperatures dropped from 200 °C to 119 °C and 245 to 186 °C, respectively.

Stress relaxation and sweep frequency experiments are widely used methods to characterize the degree of plasticity in polymer networks.[67] Accordingly, stress relaxation measurements for PPO_{900}-Bz-Bor (cured) were performed at different temperatures. The relaxation time (t) is defined as the time required to relax to $1/e$ of the initial modulus. Fig. 6 depicts the stress relaxation curves from 25 °C to 140 °C and shows a clear relaxation process of the modulus values (Fig. 6a). The relaxation modulus was normalized and plotted on a logarithmic scale. Obviously, the modulus decreases at a faster rate when the temperature is higher. Moreover, the cured PPO_{900}-Bz-Bor showed relaxation dynamics, characterized by a comparable activation energy (E_a) of 60.6 kJ mol^{-1}. This value is in the same range for the reported activation energies for boronic ester systems.[68,69] In addition to temperature dependent analyses, the cured PPO_{900}-Bz-Bor, self-healed PPO_{900}-Bz-Bor and PPO_{900}-Bz as reference materials were compared (Fig. S17†). Moreover, sweep frequency measurements (Fig. 6c and d) revealed that the elastic modulus of the self-healed sample is higher compared to those of the dried and undried PPO_{900}-Bz-Bor and PPO_{900}-Bz. Accordingly, the self-healed material has a lower relaxation time at high frequencies and is much stronger as observed by stress–strain measurements.

Apart from healing tests, the hydrolytic stability of the materials was also tested. In general, the water resistance of many polymer materials based on boronic esters could be insufficient for practical applications in a humid environment. In contrast to the stated problem, PPO_{900}-Bz-Bor showed better hydrolytic stability than conventional boronic esters because of the intramolecular B–N linkages.[68] In general, the intramolecular interactions between boron and nitrogen atoms were reported to be weak when aromatic amines were used.[70] However, the coordination between B and N atoms is expected to be stronger in PBzs as the B–N interactions occur on the Mannich bridge representing a benzylic amine structure. Accordingly, when PPO_{900}-Bz-Bor is placed in water the boronate hydrolysis becomes significant only after 5 days and the network starts to crumble by applying a force with a spatula after 9 days (Fig. 7). Unlike the PPO-Bz-Bor system, when water was added to boronic esters in a 15 : 1 molar ratio, ~97% of the boronic esters were hydrolyzed after only 30 s as reported previously.[44]

In general, boric/boronic acid added resins exhibit high thermo-oxidative stability and enhanced char yields.[71] Therefore, modified phenolic resins and a series of ablative resistant polymers have been developed for high temperature applications using boric/boronic acid and their derivatives.[40] In a similar fashion, PPO-Bz-Bor polymers are expected to have

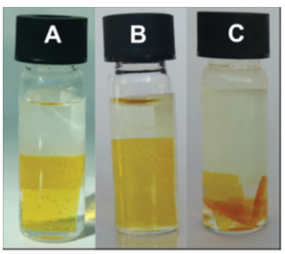

Fig. 7 PPO_{900}-Bz-Bor in water for 1 (A), 5 (B), and 9 (C) days.

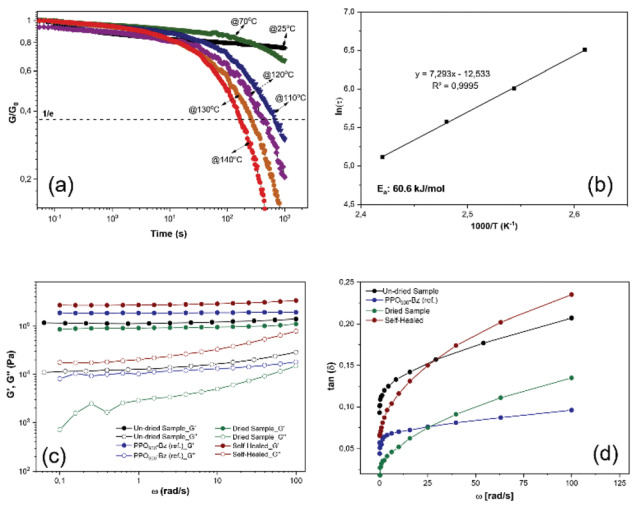

Fig. 6 Normalized relaxation module (G) *vs.* time graphs for the cured PPO_{900}-Bz-Bor at different temperatures (a), the logarithm of relaxation time ln(τ) *versus* reciprocal temperature (1000/T) (b), and the storage (G') and loss (G'') moduli are plotted as a function of frequency for the samples of dried, undried, self-healed PPO_{900}-Bz-Bor, and PPO_{900}-Bz at 25 °C (c) and (d).

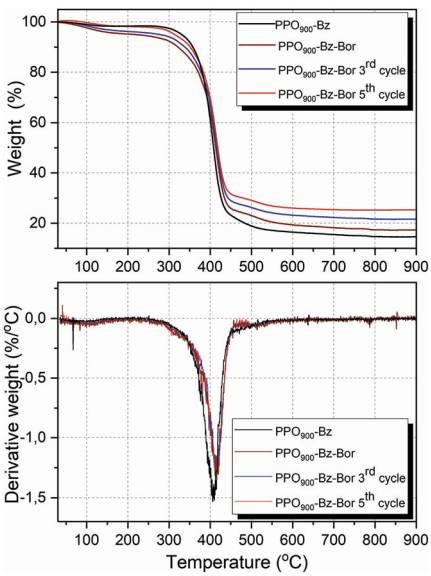

Fig. 8 TGA traces of the cured PPO_{900}-Bz, PPO_{900}-Bz-Bor and recycled PPO_{900}-Bz-Bor.

a better thermal resistance compared to PPO-Bz polymers. The thermal stability of the PPO_{900}-Bz, PPO_{900}-Bz-Bor and recycled samples was studied by thermogravimetric analysis (TGA). TGA traces and related thermo-gravimetric results are presented in Fig. 8 and Table S2.† Boronic acid modified PBz exhibited higher char yield and delayed the maximum degradation temperature (T_{max}) compared to PPO_{900}-Bz. Interestingly, after each healing cycle PPO_{900}-Bz-Bor gave higher char yields indicating the improved B–O bonding. In this way, the fragmentation of phenolic moieties was delayed, resulting in higher char yield and overall thermal stability. Actually, this behavior is well in agreement with the tensile strength results and supports the explanations for the healing efficiency increment after each cycle. Moreover, the T_{max} value for PPO_{900}-Bz-Bor remained approximately unchanged that can be considered as another clue for the B–N interaction that delays Mannich bridge degradation.

Conclusions

The structure of PBz contains free hydroxyls and nitrogen atoms available to bind boronic acids to yield boronic esters with B–N coordination bonds. Therefore, the inherent structure of PBz is quite convenient to design efficient self-healable polymers based on boronic ester exchange reactions accelerated by B–N interactions. Accordingly, in this work, the design and synthesis of self-healable/recyclable PBz networks under mild conditions, by exploiting both dynamic B–O bond exchanges and inherent supramolecular interactions of PBzs, have been reported. The cured PPO-Bz-Bor films displayed self-healing properties at low temperatures and under very mild pressures in the absence of additives to promote the healing process. Moreover, PPO_{900}-Bz-Bor showed higher hydrolysis stability than conventional boronic esters because of the intramolecular coordination of B–N in the linkages. Accordingly, when PPO_{900}-Bz-Bor was placed in water the boronate hydrolysis became significant only after 5 days.

The described approach is facile to achieve water resistant self-healable PBz containing boronic esters, since simple chemicals such as Jeffamines, bisphenol A, and formaldehyde were used for main chain PBz precursors and phenyl boronic acid for establishing dynamic bonding. In summary, this work demonstrates the capacity of benzoxazine chemistry to produce advanced materials by engineering the Mannich bridge and phenolic hydroxyls with special reagents.

Conflicts of interest

There are no conflicts to declare.

Acknowledgements

The authors thank the Istanbul Technical University Research Fund (project number: 43364) for financial support. One of the authors, S. G., would like to thank YOK for the 100/2000 Doctoral Scholarship. The authors thank Prof. Oguz Okay for providing infrastructure for tensile tests. The authors also thank Prof. Seniha Guner and Banu A. Kocaaga for rheology measurements.

Notes and references

1 N. Ghosh, B. Kiskan and Y. Yagci, *Prog. Polym. Sci.*, 2007, **32**, 1344–1391.
2 B. Kiskan and Y. Yagci, *Isr. J. Chem.*, 2020, **60**, 20–32.
3 V. Vatanpour, B. Kiskan, B. Zeytuncu and I. Koyuncu, *Sep. Purif. Technol.*, 2022, **278**, 119562.
4 H. Ishida and T. Agag, *Handbook of Benzoxazine Resins*, Elsevier, 2011.
5 L. Han, M. L. Salum, K. Zhang, P. Froimowicz and H. Ishida, *J. Polym. Sci., Part A: Polym. Chem.*, 2017, **55**, 3434–3445.
6 Y. Lu, M. Li, Y. Zhang, D. Hu, L. Me and W. Xu, *Thermochim. Acta*, 2011, **515**, 32–37.
7 J. Sun, W. Wei, Y. Xu, J. Qu, X. Liu and T. Endo, *RSC Adv.*, 2015, **5**, 19048–19057.
8 Z. Deliballi, B. Kiskan and Y. Yagci, *Polym. Chem.*, 2021, **12**, 5781–5786.
9 Z. G. Coban, Y. Yagci and B. Kiskan, *ACS Appl. Polym. Mater.*, 2021, **3**, 4203–4212.
10 B. Lochab, M. Monisha, N. Amarnath, P. Sharma, S. Mukherjee and H. Ishida, *Polymers*, 2021, **13**, 1260.
11 A. Kocaarslan, B. Kiskan and Y. Yagci, *Polymer*, 2017, **122**, 340–346.
12 M. Imran, B. Kiskan and Y. Yagci, *Tetrahedron Lett.*, 2013, **54**, 4966–4969.
13 G. Lligadas, A. Tüzün, J. C. Ronda, M. Galià and V. Cádiz, *Polym. Chem.*, 2014, **5**, 6636–6644.
14 M. G. Mohamed and S.-W. Kuo, *Macromolecules*, 2020, **53**, 2420–2429.
15 X. Zhang, M. G. Mohamed, Z. Xin and S.-W. Kuo, *Polymer*, 2020, **201**, 122552.
16 C.-F. Wang, Y.-C. Su, S.-W. Kuo, C.-F. Huang, Y.-C. Sheen and F.-C. Chang, *Angew. Chem., Int. Ed.*, 2006, **45**, 2248–2251.
17 F. S. Gungor, B. Bati and B. Kiskan, *Eur. Polym. J.*, 2019, **121**, 109352.
18 W.-H. Hu, K.-W. Huang and S.-W. Kuo, *Polym. Chem.*, 2012, **3**, 1546–1554.
19 Z. Wang, S. Yao, K. Song, X. Gong, S. Zhang, S. Gao and Z. Lu, *Green Chem.*, 2020, **22**, 3481–3488.
20 K. Zhang, M. Han, L. Han and H. Ishida, *Eur. Polym. J.*, 2019, **116**, 526–533.
21 B. Kiskan, *React. Funct. Polym.*, 2018, **129**, 76–88.
22 A. Adjaoud, L. Puchot and P. Verge, *ACS Sustainable Chem. Eng.*, 2022, **10**, 594–602.
23 X. Cao, J. Pan, G. Cai, S. Xiao, X. Ma, X. Zhang and Z. Dong, *Prog. Org. Coat.*, 2022, **163**, 106630.
24 C. Bo, Y. Sha, F. Song, M. Zhang, L. Hu, P. Jia and Y. Zhou, *J. Cleaner Prod.*, 2022, **341**, 130898.

25 B. Kiskan and Y. Yagci, *J. Polym. Sci., Part A: Polym. Chem.*, 2014, **52**, 2911–2918.
26 M. Arslan, B. Kiskan and Y. Yagci, *Macromolecules*, 2018, **51**, 10095–10103.
27 O. Taskin, B. Kiskan and Y. Yagci, *Macromolecules*, 2013, **46**, 8773–8778.
28 M. Arslan, B. Kiskan and Y. Yagci, *Sci. Rep.*, 2017, **7**, 5207–5207.
29 A. G. Simmonds, J. J. Griebel, J. Park, K. R. Kim, W. J. Chung, V. P. Oleshko, J. Kim, E. T. Kim, R. S. Glass, C. L. Soles, Y.-E. Sung, K. Char and J. Pyun, *ACS Macro Lett.*, 2014, **3**, 229–232.
30 W. J. Chung, J. J. Griebel, E. T. Kim, H. Yoon, A. G. Simmonds, H. J. Ji, P. T. Dirlam, R. S. Glass, J. J. Wie, N. A. Nguyen, B. W. Guralnick, J. Park, S. Árpád, P. Theato, M. E. Mackay, Y.-E. Sung, K. Char and J. Pyun, *Nat. Chem.*, 2013, **5**, 518–524.
31 S. Shukla, A. Ghosh, P. K. Roy, S. Mitra and B. Lochab, *Polymer*, 2016, **99**, 349–357.
32 M. Arslan, B. Kiskan and Y. Yagci, *Macromolecules*, 2016, **49**, 767–773.
33 O. Bayram, B. Kiskan, E. Demir, R. Demir-Cakan and Y. Yagci, *ACS Sustainable Chem. Eng.*, 2020, **8**, 9145–9155.
34 A. Trejo-Machin, L. Puchot and P. Verge, *Polym. Chem.*, 2020, **11**, 7026–7034.
35 A. Adjaoud, A. Trejo-Machin, L. Puchot and P. Verge, *Polym. Chem.*, 2021, **12**, 3276–3289.
36 F. Fu, M. Huang, W. Zhang, Y. Zhao and X. Liu, *Sci. Rep.*, 2018, **8**, 10325.
37 L. Zhang, Z. Zhao, Z. Dai, L. Xu, F. Fu, T. Endo and X. Liu, *ACS Macro Lett.*, 2019, **8**, 506–511.
38 S. Gao, Y. Liu, S. Feng and Z. Lu, *J. Mater. Chem. A*, 2019, **7**, 17498–17504.
39 A. P. Bapat, B. S. Sumerlin and A. Sutti, *Mater. Horiz.*, 2020, **7**, 694–714.
40 X. Zhang, Y. Zhao, S. Wang and X. Jing, *Mater. Chem. Front.*, 2021, **5**, 5534–5548.
41 S. Wu, H. Yang, W.-S. Xu and Q. Chen, *Macromolecules*, 2021, **54**, 6799–6809.
42 L. L. Robinson, J. L. Self, A. D. Fusi, M. W. Bates, J. Read de Alaniz, C. J. Hawker, C. M. Bates and C. S. Sample, *ACS Macro Lett.*, 2021, **10**, 857–863.
43 W. A. Ogden and Z. Guan, *J. Am. Chem. Soc.*, 2018, **140**, 6217–6220.
44 J. J. Cash, T. Kubo, A. P. Bapat and B. S. Sumerlin, *Macromolecules*, 2015, **48**, 2098–2106.
45 Z.-H. Zhao, D.-P. Wang, J.-L. Zuo and C.-H. Li, *ACS Mater. Lett.*, 2021, **3**, 1328–1338.
46 X. Lu, C. Bao, P. Xie, Z. Guo and J. Sun, *Adv. Funct. Mater.*, 2021, **31**, 2103061.
47 J. Gao, L. Xia and Y. Liu, *Polym. Degrad. Stab.*, 2004, **83**, 71–77.
48 M. O. Abdalla, A. Ludwick and T. Mitchell, *Polymer*, 2003, **44**, 7353–7359.
49 J. Gao, Y. Liu and F. Wang, *Eur. Polym. J.*, 2001, **37**, 207–210.
50 J. Gao, Y. Liu and L. Yang, *Polym. Degrad. Stab.*, 1999, **63**, 19–22.
51 H. Ipek and J. Hacaloglu, *J. Polym. Res.*, 2020, **27**, 245.
52 S. Wang, Q. Jia, Y. Liu and X. Jing, *React. Funct. Polym.*, 2015, **93**, 111–119.
53 B. Marco-Dufort and M. W. Tibbitt, *Mater. Today Chem.*, 2019, **12**, 16–33.
54 C. C. Deng, W. L. A. Brooks, K. A. Abboud and B. S. Sumerlin, *ACS Macro Lett.*, 2015, **4**, 220–224.
55 O. R. Cromwell, J. Chung and Z. Guan, *J. Am. Chem. Soc.*, 2015, **137**, 6492–6495.
56 C. Bao, Y.-J. Jiang, H. Zhang, X. Lu and J. Sun, *Adv. Funct. Mater.*, 2018, **28**, 1800560.
57 S. Delpierre, B. Willocq, J. De Winter, P. Dubois, P. Gerbaux and J.-M. Raquez, *Chem. – Eur. J.*, 2017, **23**, 6730–6735.
58 K. Song, W. Ye, X. Gao, H. Fang, Y. Zhang, Q. Zhang, X. Li, S. Yang, H. Wei and Y. Ding, *Mater. Horiz.*, 2021, **8**, 216–223.
59 S. Wang, B. Wang, X. Zhang, L. Wang, W. Fan, H. Li, C. Bian and X. Jing, *Appl. Surf. Sci.*, 2021, **570**, 151157.
60 S. Franzen, W. Ni and B. Wang, *J. Phys. Chem. B*, 2003, **107**, 12942–12948.
61 Y. Tsukamoto, J. Kida, D. Aoki and H. Otsuka, *Polym. Chem.*, 2021, **12**, 5266–5270.
62 A. Chernykh, J. Liu and H. Ishida, *Polymer*, 2006, **47**, 7664–7669.
63 T. Agag; and T. Takeichi, *J. Polym. Sci., Part A: Polym. Chem.*, 2007, **45**, 1878–1888.
64 T. Takeichi, T. Kano and T. Agag, *Polymer*, 2005, **46**, 12172–12180.
65 C. H. Lin, S. L. Chang, T. Y. Shen, Y. S. Shih, H. T. Lin and C. F. Wang, *Polym. Chem.*, 2012, **3**, 935–945.
66 R. P. Wool and K. M. Oconnor, *J. Appl. Phys.*, 1981, **52**, 5953–5963.
67 C. J. Kloxin and C. N. Bowman, *Chem. Soc. Rev.*, 2013, **42**, 7161–7173.
68 X. Zhang, S. Wang, Z. Jiang, Y. Li and X. Jing, *J. Am. Chem. Soc.*, 2020, **142**, 21852–21860.
69 Y. Yang, F.-S. Du and Z.-C. Li, *Polym. Chem.*, 2020, **11**, 1860–1870.
70 Y. Ito, J. Kida, D. Aoki and H. Otsuka, *Chem. Commun.*, 2018, **54**, 12930–12933.
71 J. Yun, L. Chen, H. Zhao, X. Zhang, W. Ye and D. Zhu, *Macromol. Rapid Commun.*, 2019, **40**, 1800702.